

## A wave-based computational method for free vibration and buckling analysis of rectangular Reddy nanoplates

A.Zargaripoor<sup>a\*</sup>, M.Nikkhah Bahrami<sup>a</sup>

<sup>a</sup> School of Mechanical Engineering, College of Engineering, University of Tehran, Tehran, Iran

### ARTICLE INFO

#### Article history:

Received: 07 April 2018  
Accepted: 23 May 2018

#### Keywords:

Rectangular thick nanoplate  
Propagation matrix  
Reflection matrix  
Vibration analysis  
Buckling analysis

### ABSTRACT

In this paper, the wave propagation method is combined with nonlocal elasticity theory to analyze the buckling and free vibration of rectangular Reddy nanoplate. Wave propagation is one of the powerful methods for analyzing the vibration and buckling structures. It is assumed that the plate has two opposite edges simply supported and the other two edges may be simply supported or clamped. It is the first time that the wave propagation method is used for thick nanoplates. In this study, firstly the matrices of propagation and reflection are derived. Then, these matrices are combined to propose an exact method for obtaining the natural frequencies and critical buckling loads which can be useful for future studies. It is observed that the obtained results of the wave propagation method are in good agreement with the obtained values by literature. At the end, the obtained results are presented to evaluate the influence of different parameters such as nonlocal parameter, aspect ratio and thickness to length ratio of nanoplate.

### 1. Introduction

Nowadays nanoplates have been used widely in nano-sensors and nano-resonators. In the nanostructure, the internal characteristic length scale is comparable to the size of systems. As a result, for an accurate modeling, the atomic forces should be considered to account, which theories of classical continuum mechanics cannot consider these forces. Recently several non-classical theories such as couple stress [1], strain gradient [2] and nonlocal theory [3] try to capture the size effect. Among these methods nonlocal theory has been used widely. In the classical theories of continuum mechanics, the stress in a point is related only to the strain in that specific point; however, in the nonlocal theory, the stress is related to the strain in the whole of the volume. Eringen [4] presented this theory and used it in different problems.

Many researches have contributed to study the vibration and buckling analysis of macro and nanoplates [5-7]. Pradhan and Phadikar [8] reformulated classical plate theory and first-order shear deformation theory of plates using the nonlocal differential constitutive relations of Eringen. Murmu and Pradhan [9] investigated small-scale effects on the free in-plane vibration of nanoplates employing nonlocal continuum mechanics. Aghababaei and Reddy [10] presented analytical solutions of bending and free vibration of a simply supported rectangular plate using the nonlocal linear elasticity theory of Eringen to illustrate the effect of nonlocal theory on deflection and natural frequency of the plates. Aksencer and Aydogdu [11] studied buckling and vibration of nanoplates using nonlocal elasticity theory. Malekzadeh and Shojaee [12] extended the application of a two-

variable refined plate theory to the free vibration of nanoplates. Chakraverty and Behera [13] considered vibration analysis of isotropic rectangular nanoplates based on the classical plate theory in conjunction with Eringen's nonlocal elasticity theory. They used Rayleigh-Ritz method with algebraic polynomial displacement function to solve the vibration problem of isotropic rectangular nanoplates subjected to different boundary conditions. Malekzadeh and Shojaee [14] employed a two-variable first-order shear deformation theory in combination with surface free energy and small scale to present a simple and computationally efficient formulation for the free vibration of nanoplates with arbitrary boundary conditions. Chakraverty and Behera [15] studied free vibration of non-uniform embedded nanoplates based on classical plate theory in conjunction with nonlocal elasticity theory. Panyatong et al. [16] developed the second-order shear deformation plate theory for the study of the natural frequencies of rectangular nanoplates based on the nonlocal elasticity theory of Eringen. Behera and Chakraverty [17] applied the Rayleigh-Ritz method to solve governing differential equations of the free vibration of nonhomogeneous rectangular nanoplates. Faroughi and Goushegir [18] employed the Ritz method to analyze the free in-plane vibration of heterogeneous rectangular nanoplates corresponding to Eringen's nonlocal elasticity theory. Karimi et al. [19] used finite difference method to study the size-dependent free vibration characteristics of rectangular nanoplates considering the surface stress effects. Sarrami-Foroushani and Azhari [20] analyzed the buckling and vibration of thick rectangular nanoplates. Hosseini-Hashemi et al. [21] presented analytical closed-form solutions in explicit forms to investigate small scale effects on the buckling and the transverse vibration behavior of

\* Corresponding Author. . Tel.: +98 126064537; Fax: +98 21 44648239 Email Address: [alizargaripoor@ut.ac.ir](mailto:alizargaripoor@ut.ac.ir)

Levy-type rectangular nanoplates based on Reddy's nonlocal third-order shear deformation plate theory. Rong et al. [22] proposed an analytical Hamiltonian-based model for the dynamic analysis of rectangular nanoplates using the Kirchhoff plate theory and Eringen's nonlocal theory. Daneshmehr et al. [23] investigated the free vibration behavior of the nanoplate made of functionally graded materials with small-scale effects. The generalized differential quadrature method (GDQM) was used to solve the governing equations for various boundary conditions to obtain the nonlinear natural frequencies of FG nanoplates. Hosseini et al. [24] studied stress distribution in a single-walled carbon nanotube under internal pressure with various chirality. Hosseini et al. [25] presented the stress analysis of rotating nano-disk of functionally graded materials with nonlinearly varying thickness based on strain gradient theory. Zamani Nejad et al. [26] used a semi-analytical iterative method as one of the newest analytical methods for the elastic analysis of thick-walled spherical pressure vessels made of functionally graded materials subjected to internal pressure. In other work, Zamani Nejad and Hadi [27] formulated the problem of the static bending of Euler-Bernoulli nano-beams made of bi-directional functionally graded material with small scale effects. Also, Zamani Nejad and Hadi [28] investigated the free vibration analysis of Euler-Bernoulli nano-beams made of bi-directional functionally graded material with small scale effects. Zamani Nejad et al. [29] presented consistent couple-stress theory for free vibration analysis of Euler-Bernoulli nano-beams made of arbitrary bi-directional functionally graded materials. Also, Zamani Nejad et al. [30] presented buckling analysis of the nano-beams made of two-directional functionally graded materials with small scale effects based on nonlocal elasticity theory. In other work, Zamani Nejad et al. [31] presented an exact closed-form analytical solution for elasto-plastic deformations and stresses in a rotating disk made of functionally graded materials in which the elasto-perfectly-plastic material model is employed. Shishesaz et al. [32] studied the thermoelastic behavior of a functionally graded nanodisk based on the strain gradient theory. Hadi et al. [33] presented buckling analysis of FGM Euler-Bernoulli nano-beams with 3D-varying properties based on consistent couple-stress theory. Zamani Nejad et al. [34] discussed some critical issues and problems in the development of thick shells made from functionally graded piezoelectric material. Hadi et al. [35] presented an investigation on the free vibration of three-directional functionally graded material Euler-Bernoulli nano-beam, with small scale effects.

Even though there are some classical analytical and exact solutions of the nonlocal plate theory, in these method the natural frequencies are obtained by applying the boundary conditions to the general solution of differential equation. There is an alternative approach called wave propagation method, which considers vibrations as propagating waves traveling in the structures.

Zhang and Lam [36] presented the vibration analysis of cylindrical shells using wave propagation method. Mei and Mace [37] presented wave reflection, transmission and propagation in Timoshenko beams with wave analysis of vibrations in Timoshenko beam structures. Natsuki and Endo [38] presented a vibration analysis of single-and double-walled carbon nanotubes as well as nanotubes embedded in an elastic matrix using wave propagation approach. Xuebin [39] presented a wave propagation approach for free analysis of circular cylindrical shell, based on Fluge classical thin shell theory. Bahrami et al. [40] analyzed the free vibration of annular circular and sectorial membranes using wave propagation approach. In other work, Bahrami and Teimourian [41] combined the wave propagation approach with

nonlocal elasticity theory to analyze the buckling and free vibration of Euler-Bernoulli nanobeams. Ilkhani et al. [42] used wave propagation approach to analyze the free vibrations analysis of thin rectangular macro and nano-plates. Bahrami and Teimourian [43] presented the wave propagation approach for analyzing the free vibration and wave reflection in carbon nanotubes. Also, they presented the wave propagation approach for free vibration analysis of non-uniform annular and circular membranes [41]. Recently, Bahrami and Teimourian [44] presented the wave propagation approach for free vibration analysis of non-uniform rectangular membranes. Moreover, Bahrami and Teimourian [45] developed the wave propagation technique for analyzing the wave power reflection in circular annular nanoplates. In other work, Bahrami [46] utilized the wave propagation method and the differential constitutive law consequent to the Eringen strain-driven integral nonlocal elasticity model to analyze the free vibration, wave power transmission and reflection in multi-cracked nanorods. Also, Bahrami [44] utilized the wave propagation method and the nonlocal elasticity theory to analyze the vibration, wave power transmission and reflection in multi-cracked Euler-Bernoulli nanobeams.

According to present literature review, the wave propagation method for thick nanoplates has not been addressed. In addition, there were at most two waves in analyzing all the above-mentioned structures while in this study, there are four waves for the first time causing the problem to be more complicated to analyze. In this study, firstly the matrices of propagation and reflection are derived and by combining them, the characteristic equation of the plate is obtained.

## 2. Modeling and Formulation

### 2.1 Non-local elasticity theory

Non-local elastic theory which introduced by Eringen [4] is one of the unconventional contemporary theories that the effects of small scales are applied in the characteristic equations of this theory. In the nonlocal theory, the stress tensor in the point  $\mathbf{x}$  of a physical environment  $\Omega$  is connected to the strain tensor  $\boldsymbol{\varepsilon}$  in whole of the environment by an integral equation. In other words, constitutive law of nonlocal theory is

$$\boldsymbol{\sigma}(\mathbf{x}) = \iiint \alpha(|\mathbf{x}' - \mathbf{x}|, \tau) \mathbf{C} \boldsymbol{\varepsilon}(\mathbf{x}') d\mathbf{v} \quad (1)$$

Element  $\alpha(|\mathbf{x}' - \mathbf{x}|, \tau)$  is called nonlocal modulus and acts as a weight function in this equation.  $|\mathbf{x}' - \mathbf{x}|$  is distance between local and nonlocal point.  $\mathbf{C}$  is fourth-order tensor which exists in classical theory too.  $\eta$  is related to the internal length scale ( $\bar{a}$ ) and outer length scale ( $l$ ) as

$$\eta = \frac{e_0 \bar{a}}{l} = \sqrt{\frac{\mu}{l^2}} \quad (2)$$

which  $e_0$  is a physical parameter that has been identified by experimental results. And the parameter  $\mu = (e_0 \bar{a})^2$  is called small size parameter.

At last the form of structural equation of non-localized elastic theory is as follows.

$$(1 - \mu \nabla^2) \sigma = C : \varepsilon \quad (3)$$

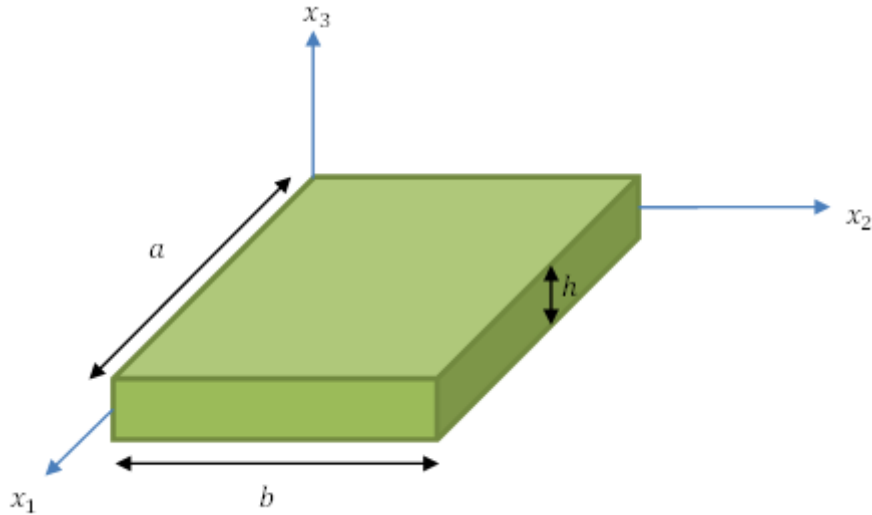


Figure 1. Geometry of rectangular isotropic thick plate

It should be mentioned, when the body is not small; consequently, the small size parameter is small, the nonlocal constitutive parameter converges to the classical theory.

### 2.2 Governing Equations of motion

In Figure 1, a thick isotropic rectangular plate is shown with length  $a$ , width  $b$  and height  $h$ . In Reddy plate theory[47], the displacement components are presumed to be given as:

$$u(x_1, x_2, x_3, t) = u_0(x_1, x_2, t) + x_3 \varphi_1(x_1, x_2, t) - \frac{4x_3^3}{3h^2} \left( \varphi_1 + \frac{\partial w_0}{\partial x_1} \right) \quad (4a)$$

$$v(x_1, x_2, x_3, t) = v_0(x_1, x_2, t) + x_3 \varphi_2(x_1, x_2, t) - \frac{4x_3^3}{3h^2} \left( \varphi_2 + \frac{\partial w_0}{\partial x_2} \right) \quad (4b)$$

$$w(x_1, x_2, x_3, t) = w_0(x_1, x_2, t) \quad (4c)$$

where  $u, v$  and  $w$  are the mid-plane displacements and  $\varphi_1$  and  $\varphi_2$  show normal rotation perpendicular to middle of the plate around  $x_2$  and  $x_1$  axes, respectively.

By using the above displacement fields, the strain equation could be written as follows:

$$\varepsilon_{11} = \frac{\partial u_0(x_1, x_2, t)}{\partial x_1} + x_3 \frac{\partial \varphi_1(x_1, x_2, t)}{\partial x_1} - \frac{4}{3h^2} x_3^3 \left( \frac{\partial \varphi_1}{\partial x_1} + \frac{\partial^2 w_0}{\partial x_1^2} \right) \quad (5a)$$

$$\varepsilon_{22} = \frac{\partial v_0(x_1, x_2, t)}{\partial x_2} + x_3 \frac{\partial \varphi_2(x_1, x_2, t)}{\partial x_2} - \frac{4}{3h^2} x_3^3 \left( \frac{\partial \varphi_2}{\partial x_2} + \frac{\partial^2 w_0}{\partial x_2^2} \right) \quad (5b)$$

$$\varepsilon_{33} = 0 \quad (5c)$$

$$\varepsilon_{12} = \frac{1}{2} \left( \frac{\partial u_0(x_1, x_2, t)}{\partial x_2} + \frac{\partial v_0(x_1, x_2, t)}{\partial x_1} \right) + x_3 \left( \frac{\partial \varphi_1(x_1, x_2, t)}{\partial x_2} + \frac{\partial \varphi_2(x_1, x_2, t)}{\partial x_1} \right) \quad (5d)$$

$$- \frac{4}{3h^2} x_3^3 \left( \frac{\partial \varphi_1}{\partial x_2} + 2 \times \frac{\partial^2 w_0}{\partial x_1 \partial x_2} + \frac{\partial \varphi_2}{\partial x_1} \right)$$

$$\varepsilon_{13} = \frac{1}{2} \left( 1 - \frac{4}{h^2} x_3^2 \right) \left( \varphi_1 + \frac{\partial w_0(x_1, x_2, t)}{\partial x_1} \right) \quad (5e)$$

$$\varepsilon_{23} = \frac{1}{2} \left( 1 - \frac{4}{h^2} x_3^2 \right) \left( \varphi_2 + \frac{\partial w_0(x_1, x_2, t)}{\partial x_2} \right) \quad (5f)$$

So the stress-strain relations for the plane stress problem are defined as:

$$\begin{bmatrix} \sigma_{11} \\ \sigma_{22} \\ \sigma_{12} \\ \sigma_{23} \\ \sigma_{13} \end{bmatrix} = \frac{E}{1-\nu^2} \begin{bmatrix} u_{0,1} + \nu v_{0,2} \\ v_{0,1} + \nu u_{0,1} \\ \frac{1-\nu}{2}(u_{0,2} + v_{0,1}) \\ \frac{1-\nu}{2}(\varphi_2 + w_{,2}) \\ \frac{1-\nu}{2}(\varphi_1 + w_{,1}) \\ \frac{4x_3^3}{h^2} \frac{1-\nu}{2}(\varphi_{1,1} + w_{,11}) + \nu(\varphi_{2,2} + w_{,22}) \\ \frac{4x_3^3}{h^2} \frac{1-\nu}{2}(\varphi_{2,2} + w_{,22}) + \nu(\varphi_{1,1} + w_{,11}) \\ \frac{4x_3^3}{h^2} \frac{1-\nu}{2}(\varphi_{1,2} + \varphi_{2,1} + 2w_{,12}) \\ 0 \\ 0 \end{bmatrix} + x_3 \begin{bmatrix} \varphi_{1,1} + \nu \varphi_{2,2} \\ \varphi_{2,2} + \nu \varphi_{1,1} \\ \frac{1-\nu}{2}(\varphi_{1,2} + \varphi_{2,1}) \\ 0 \\ 0 \end{bmatrix} - \frac{4x_3^2}{h^2} \begin{bmatrix} 0 \\ 0 \\ 0 \\ \frac{1-\nu}{2}(\varphi_2 + w_{,2}) \\ \frac{1-\nu}{2}(\varphi_1 + w_{,1}) \end{bmatrix} \quad (6)$$

where  $E$  is the Young modulus of elasticity and  $\nu$  is the Poisson's ratio.

By using displacement field in Hamilton principle and according to the same approach used by [10], the equations of motion based on forces and moments are achieved as follows:

$$\delta u_0 : \frac{\partial N_1}{\partial x_1} + \frac{\partial N_6}{\partial x_2} = (1 - \mu \nabla^2)(I_1 \frac{\partial^2 u_0}{\partial t^2} + (I_2 - \frac{4}{3h^2} I_4) \frac{\partial^2 \varphi_1}{\partial t^2} - \frac{4}{3h^2} I_4 \frac{\partial^3 w_0}{\partial t^2 \partial x_1}) \quad (7a)$$

$$\delta v_0 : \frac{\partial N_2}{\partial x_2} + \frac{\partial N_6}{\partial x_1} = (1 - \mu \nabla^2)(I_1 \frac{\partial^2 v_0}{\partial t^2} + (I_2 - \frac{4}{3h^2} I_4) \frac{\partial^2 \varphi_2}{\partial t^2} - \frac{4}{3h^2} I_4 \frac{\partial^3 w_0}{\partial t^2 \partial x_2}) \quad (7b)$$

$$\delta w_0 : (\frac{4}{3h^2})(\frac{\partial^2 P_1}{\partial x_1^2} + 2 \frac{\partial^2 P_6}{\partial x_1 \partial x_2} + \frac{\partial^2 P_2}{\partial x_2^2}) + \frac{\partial Q_1}{\partial x_1} + \frac{\partial Q_2}{\partial x_2} - \frac{4}{h^2} (\frac{\partial R_1}{\partial x_1} + \frac{\partial R_2}{\partial x_2}) \quad (7c)$$

$$+ (1 - \mu \nabla^2)(N_{xx} \frac{\partial^2 w_0}{\partial x_1^2} + N_{yy} \frac{\partial^2 w_0}{\partial x_2^2}) =$$

$$(1 - \mu \nabla^2)(I_1 \frac{\partial^3 w_0}{\partial t^2} + (\frac{4}{3h^2})(I_5 - \frac{4}{3h^2} I_7) (\frac{\partial^3 \varphi_1}{\partial t^2 \partial x_1} + \frac{\partial^3 \varphi_2}{\partial t^2 \partial x_2}))$$

$$- (\frac{4}{3h^2})^2 I_7 (\frac{\partial^4 w_0}{\partial t^2 \partial x_1^2} + \frac{\partial^4 w_0}{\partial t^2 \partial x_2^2}) + (\frac{4}{3h^2}) I_4 (\frac{\partial^3 u_0}{\partial t^2 \partial x_1} + \frac{\partial^3 v_0}{\partial t^2 \partial x_2})$$

$$\delta \varphi_1 : \frac{\partial M_1}{\partial x_1} + \frac{\partial M_6}{\partial x_2} - (\frac{4}{3h^2})(\frac{\partial P_1}{\partial x_1} + \frac{\partial P_6}{\partial x_2}) - Q_1 + \frac{4}{h^2} R_1 = \quad (7d)$$

$$(1 - \mu \nabla^2)((I_2 - \frac{4}{3h^2} I_4) \frac{\partial^2 u_0}{\partial t^2} + (I_3 - \frac{8}{3h^2} I_5 + \frac{16}{9h^4} I_7) \frac{\partial^2 \varphi_1}{\partial t^2} - \frac{4}{3h^2} (I_5 - \frac{4}{3h^2} I_7) \frac{\partial^2 w_0}{\partial t^2 \partial x_1})$$

$$\delta \varphi_2 : \frac{\partial M_2}{\partial x_2} + \frac{\partial M_6}{\partial x_1} - (\frac{4}{3h^2})(\frac{\partial P_2}{\partial x_2} + \frac{\partial P_6}{\partial x_1}) - Q_2 + \frac{4}{h^2} R_2 \quad (7e)$$

$$= (1 - \mu \nabla^2)((I_2 - \frac{4}{3h^2} I_4) \frac{\partial^2 v_0}{\partial t^2} + (I_3 - \frac{8}{3h^2} I_5 + \frac{16}{9h^4} I_7) \frac{\partial^2 \varphi_2}{\partial t^2} - \frac{4}{3h^2} (I_5 - \frac{4}{3h^2} I_7) \frac{\partial^2 w_0}{\partial t^2 \partial x_2})$$

where

$$\begin{bmatrix} I_1 \\ I_2 \\ I_3 \\ I_4 \\ I_5 \\ I_6 \\ I_7 \end{bmatrix} = \int_{-h/2}^{h/2} \begin{bmatrix} 1 \\ x_3 \\ x_3^2 \\ x_3^3 \\ x_3^4 \\ x_3^5 \\ x_3^6 \end{bmatrix} \rho dx_3 \quad (8)$$

$N_{xx}$  and  $N_{yy}$  are compressive load in  $x_1$  and  $x_2$  directions.

Also, the stress resultants are defined by:

$$(N_i, M_i, P_i) = \int_{-h/2}^{h/2} \sigma_i(1, x_3, x_3^3) dx_3 \quad (i=1,2,6) \quad (9a)$$

$$(Q_2, R_2) = \int_{-h/2}^{h/2} \sigma_4(1, x_3^2) dx_3 \quad (9b)$$

$$(Q_1, R_1) = \int_{-h/2}^{h/2} \sigma_5(1, x_3^2) dx_3 \quad (9c)$$

$$\sigma_{11} = \sigma_1, \sigma_{22} = \sigma_2, \sigma_{23} = \sigma_4, \sigma_{13} = \sigma_5, \sigma_{12} = \sigma_6$$

Since the present paper deals with the out-of-plane vibration and buckling of isotropic rectangular plates, the initial in-plane displacements  $u_0$  and  $v_0$  must be zero in Eqs. (4a-c). By taking  $I_2 = I_4 = 0$ , the coupling between Eqs. (7a) and (7b) is omitted. By replacing Eqs (8) and (9a-c) into Eqs. (7c-e) and using non-dimensional terms, the dimensionless equations of motion based

on third-order shear deformation plate theory for a thick rectangular plates are [21]:

$$\begin{aligned} & [(\frac{68}{210}(1-\nu) - \frac{17}{315}\xi^2\tau^2\beta^2)\nabla^2\bar{\varphi}_1 + \frac{68}{210}(1+\nu)(\bar{\varphi}_{1,11} + \bar{\varphi}_{2,12}) \\ & - (\frac{16}{105} - \frac{4}{315}\xi^2\tau^2\beta^2)\nabla^2\bar{w}_{,1} \\ & - \frac{16}{5\tau^2}(1-\nu)(\bar{\varphi}_1 + \bar{w}_{,1})] = -\frac{17}{315}\tau^2\beta^2\bar{\varphi}_1 + \frac{4}{315}\tau^2\beta^2\bar{w}_{,1} \end{aligned} \quad (10a)$$

$$\begin{aligned} & [(\frac{68}{210}(1-\nu) - \frac{17}{315}\xi^2\tau^2\beta^2)\nabla^2\bar{\varphi}_2 + \frac{68}{210}(1+\nu)(\bar{\varphi}_{2,22} + \bar{\varphi}_{1,12}) \\ & - (\frac{16}{105} - \frac{4}{315}\xi^2\tau^2\beta^2)\nabla^2\bar{w}_{,2} \\ & - \frac{16}{5\tau^2}(1-\nu)(\bar{\varphi}_2 + \bar{w}_{,2})] = -\frac{17}{315}\tau^2\beta^2\bar{\varphi}_2 + \frac{4}{315}\tau^2\beta^2\bar{w}_{,2} \end{aligned} \quad (10b)$$

$$\begin{aligned} & (\frac{16}{105} - \frac{4}{315}\xi^2\tau^2\beta^2)\nabla^2(\bar{\varphi}_{1,1} + \bar{\varphi}_{2,2}) - (\frac{1}{21} + \frac{1}{252}\xi^2\tau^2\beta^2)\nabla^4\bar{w} \\ & + \frac{16}{5\tau^2}(1-\nu)(\bar{\varphi}_{1,1} + \bar{\varphi}_{2,2}) + (\frac{16}{5\tau^2}(1-\nu) + N - \xi^2\beta^2)\nabla^2\bar{w} = \\ & -\beta^2\bar{w} + \frac{1}{252}\tau^2\beta^2\nabla^2\bar{w} - \frac{4}{315}\tau^2\beta^2(\bar{\varphi}_{1,1} + \bar{\varphi}_{2,2}) \end{aligned} \quad (10c)$$

A comma followed by 1, 2 or 3 denotes the partial derivatives with respect to the normalized coordinates ( $\bar{X}_1 = \frac{x_1}{a}$ ,  $\bar{X}_2 = \frac{x_2}{b}$ ).  $\bar{w}$  is non-dimensional transverse displacement,  $\bar{\varphi}_1$  and  $\bar{\varphi}_2$  are non-dimensional slope due to bending alone in the respective planes which are defined by the following relations:

$$\bar{\varphi}_1(X_1, X_2, t) = \varphi_1(x_1, x_2)e^{-i\omega t} \quad (11a)$$

$$\bar{\varphi}_2(X_1, X_2, t) = \varphi_2(x_1, x_2)e^{-i\omega t} \quad (11b)$$

$$\bar{w}(X_1, X_2, t) = \frac{w(x_1, x_2)e^{-i\omega t}}{a} \quad (11c)$$

where  $\omega$  is the natural frequency of the plate.

Also the non-dimensional variables such as nonlocal parameter  $\xi$ , thickness to length ratio  $\tau$ , aspect ratio  $\delta$ , frequency parameter

$\beta$ , buckling load  $N$  and the coefficient  $f$  are defined as follows:

$$\tau = \frac{h}{a}, \delta = \frac{b}{a}, \beta = \omega a^2 \sqrt{\frac{\rho h}{D}}, N = \frac{a^2}{D} N_{xx}, f = \frac{N_{yy}}{N_{xx}}, \xi^2 = \frac{\mu}{a^2} \quad (12)$$

where  $D = \frac{Eh^3}{12(1-\nu^2)}$  and the coefficient  $f$  is set to be 1.

### 3. Solving by the wave propagation method

Solving the governing equations on the Reddy plate can be obtained by expressing the dimensionless functions  $\bar{\varphi}_1$ ,  $\bar{\varphi}_2$  and  $\bar{w}$  in the form of the dimensionless functions of potential  $W_1, W_2, W_3$  and  $W_4$  as follows [21]:

$$\bar{\varphi}_1 = C_1W_{1,1} + C_2W_{2,1} + C_3W_{3,1} + W_{4,2} \quad (13a)$$

$$\bar{\varphi}_2 = C_1W_{1,2} + C_2W_{2,2} + C_3W_{3,2} + W_{4,1} \quad (13b)$$

$$\bar{w} = W_1 + W_2 + W_3 \quad (13c)$$

where

$$C_i = \frac{-16(1-\nu) - \frac{4\tau^2\beta^2}{315} + \alpha_i^2(\frac{16}{105} - \frac{4}{315}\xi^2\tau^2\beta^2)}{\alpha_i^2(\frac{68}{105} - \frac{17}{315}\xi^2\tau^2\beta^2) + \frac{16(1-\nu)}{5\tau^2} - \frac{17\beta^2\tau^2}{315}} \quad (i=1,2,3) \quad (14)$$

Based on these considered potential functions, if the plate equations are rewritten, the differential equations will be the so-called decoupled for these functions:

$$\nabla^2W_1 + \alpha_1^2W_1 = 0, \nabla^2W_2 + \alpha_2^2W_2 = 0, \nabla^2W_3 + \alpha_3^2W_3 = 0 \quad (15)$$

In which  $\alpha_1^2, \alpha_2^2$  and  $\alpha_3^2$  can be obtained by solving the following equation:

$$y^3 + a_1y^2 + a_2y + a_3 = 0 \quad (16)$$

where

$$a_1 = -\frac{4(32\beta^2\tau^4\xi^2 - 5355\beta^4\tau^4\xi^4 + 10710N\beta^2\tau^4\xi^2 - 23940\nu\tau^2\xi^2 + 126\beta^2\tau^4 + 88200\beta^2\tau^2\xi^2) + 317520N\xi^2(\nu-1) - 64260N\tau^2 + 317520(\nu-1)}{\tau^2(149\beta^2\tau^2\xi^2 + 21420N\xi^2 + 252)(\beta^2\tau^2\xi^2 - 12)} \quad (17a)$$

$$a_2 = \frac{21(-\beta^4\tau^6 - 2040\beta^4\tau^4\xi^2 + 1020N\beta^2\tau^4 - 5040\beta^2\nu\tau^2 - 60480\beta^2\nu\xi^2 + 17280\beta^2\tau^2 + 60480\beta^2\xi^2 + 60480N(\nu-1))}{\tau^2(149\beta^2\tau^2\xi^2 + 21420N\xi^2 + 252)(\beta^2\tau^2\xi^2 - 12)} \quad (17b)$$

$$a_3 = -\frac{1260\beta^2(17\beta^2\tau^4 + 1008(\nu-1))}{\tau^2(149\beta^2\tau^2\xi^2 + 21420N\xi^2 + 252)(\beta^2\tau^2\xi^2 - 12)} \quad (17c)$$

Also:

$$\nabla^3 W_4 + \alpha_4^3 W_4 = 0 \quad (18)$$

$$\alpha_4^2 = \frac{17\tau^4\beta^2 - 1008(1-\nu)}{102(1-\nu)\tau^2} \quad (19)$$

Using the method of separation of variables, an answer set is obtained for equations (15) and (18):

$$W_1 = [A_1 \sin h(\lambda_1 X_2) + A_2 \cosh(\lambda_1 X_2)] \sin(\mu_1 X_1) + [B_1 \sin h(\lambda_1 X_2) + B_2 \cos h(\lambda_1 X_2)] \cos(\mu_1 X_1) \quad (20a)$$

$$W_2 = [A_3 \sinh(\lambda_2 X_2) + A_4 \cosh(\lambda_2 X_2)] \sin(\mu_2 X_1) + [B_3 \sinh(\lambda_2 X_2) + B_4 \cosh(\lambda_2 X_2)] \cos(\mu_2 X_1) \quad (20b)$$

$$W_3 = [A_5 \sin(\lambda_3 X_2) + A_6 \cos(\lambda_3 X_2)] \sin(\mu_3 X_1) + [B_5 \sin(\lambda_3 X_2) + B_6 \cos(\lambda_3 X_2)] \cos(\mu_3 X_1) \quad (20c)$$

$$W_4 = [A_7 \sinh(\lambda_4 X_2) + A_8 \cosh(\lambda_4 X_2)] \cos(\mu_4 X_1) + [B_7 \sinh(\lambda_4 X_2) + B_8 \cosh(\lambda_4 X_2)] \sin(\mu_4 X_1) \quad (20d)$$

In which  $A_i$  and  $B_i$  are the arbitrary constants and  $\lambda_i$  and  $\mu_i$  which are the wave numbers in two directions of  $X_2$  and  $X_1$ , are depended on  $\alpha_i$ :

$$\alpha_1^2 = \mu_1^2 + \lambda_1^2 \quad \mu_1^2 > 0 \quad \lambda_1^2 < 0 \quad (21a)$$

$$\alpha_2^2 = \mu_2^2 + \lambda_2^2 \quad \mu_2^2 > 0 \quad \lambda_2^2 < 0 \quad (21b)$$

$$\alpha_3^2 = \mu_3^2 + \lambda_3^2 \quad \mu_3^2 > 0 \quad \lambda_3^2 > 0 \quad (21c)$$

$$\alpha_4^2 = \mu_4^2 + \lambda_4^2 \quad \mu_4^2 > 0 \quad \lambda_4^2 < 0 \quad (21d)$$

Based on the third-order shear theory, the boundary conditions for two parallel corners (for example  $X_1 = 0$  and  $X_1 = 1$ ) are as follows:

Simply supported:

$$\overline{M}_2 = \overline{\varphi}_1 = \overline{w} = \overline{P}_2 = 0 \quad (22)$$

Clamped:

$$\overline{\varphi}_1 = \overline{\varphi}_2 = \overline{w} = \overline{w}_{,2} = 0 \quad (23)$$

In which:

$$\overline{M}_1 = \frac{aM_1}{12D}; \quad \overline{P}_2 = \frac{aP_2}{12h^2D}; \quad (24)$$

Now, by considering the simply support conditions in the corners  $X_1 = 0$  and  $X_1 = 1$  and applying our wave answers to these support conditions, answers can be written as follows:

$$\mu_1 = \mu_2 = \mu_3 = m\pi \quad (25)$$

$$W_1 = [A_1 \sinh(\lambda_1 X_2) + A_2 \cos h(\lambda_1 X_2)] \sin(m\pi X_1) \quad (26a)$$

$$W_2 = [A_3 \sinh(\lambda_2 X_2) + A_4 \cosh(\lambda_2 X_2)] \sin(m\pi X_1) \quad (26b)$$

$$W_3 = [A_5 \sin(\lambda_3 X_2) + A_6 \cos(\lambda_3 X_2)] \sin(m\pi X_1) \quad (26c)$$

$$W_4 = [A_7 \sinh(\lambda_4 X_2) + A_8 \cosh(\lambda_4 X_2)] \cos(m\pi X_1) \quad (26d)$$

By substituting the formulas  $W_i$  in equations related to potential function and considering the following equations,  $\overline{\varphi}_i$  can be obtained:

$$\sin(\theta) = \frac{e^{i\theta} - e^{-i\theta}}{2i}; \quad \cos(\theta) = \frac{e^{i\theta} + e^{-i\theta}}{2}; \quad (27)$$

$$\sinh(\theta) = \frac{e^\theta - e^{-\theta}}{2}; \quad \cosh(\theta) = \frac{e^\theta + e^{-\theta}}{2}$$

Which we will have:

$$\bar{\varphi}_1 = [A_1' C_1 m \pi e^{\lambda_1 X_2} + A_2' C_1 m \pi e^{-\lambda_1 X_2} + A_3' C_2 m \pi e^{\lambda_2 X_2} + A_4' C_2 m \pi e^{-\lambda_2 X_2} + A_5' C_3 m \pi e^{i \lambda_3 X_2} + A_6' C_3 m \pi e^{-i \lambda_3 X_2} + A_7' \lambda_4 e^{\lambda_4 X_2} + A_8' \lambda_4 e^{-\lambda_4 X_2}] \cos(m \pi X_1) \quad (28a)$$

$$\bar{\varphi}_2 = [A_1'' C_1 \lambda_4 e^{\lambda_4 X_2} + A_2'' C_1 \lambda_4 e^{-\lambda_4 X_2} + A_3'' C_2 \lambda_2 e^{\lambda_2 X_2} + A_4'' C_2 \lambda_2 e^{-\lambda_2 X_2} + A_5'' C_3 \lambda_3 e^{i \lambda_3 X_2} + A_6'' C_3 \lambda_3 e^{-i \lambda_3 X_2} + A_7'' m \pi e^{\lambda_4 X_2} + A_8'' m \pi e^{-\lambda_4 X_2}] \sin(m \pi X_1) \quad (28b)$$

$$\bar{w} = [A_1''' e^{\lambda_1 X_2} + A_2''' e^{-\lambda_1 X_2} + A_3''' e^{\lambda_2 X_2} + A_4''' e^{-\lambda_2 X_2} + A_5''' e^{i \lambda_3 X_2} + A_6''' e^{-i \lambda_3 X_2}] \sin(m \pi X_1) \quad (28c)$$

In which:

$$A_1' = \frac{A_1 + A_2}{2}; A_2' = \frac{A_2 - A_1}{2}; A_3' = \frac{A_3 + A_4}{2} \quad (29a)$$

$$A_4' = \frac{A_4 + A_3}{2}; A_5' = \frac{A_6 - i A_5}{2}; A_6' = \frac{i A_5 + A_6}{2} \quad (29b)$$

$$A_7' = \frac{A_7 + A_8}{2}; A_8' = \frac{A_7 - A_8}{2} \quad (29c)$$

As it can be seen, in the equations above,  $A_i''$  and  $A_i'''$  can be written based on  $A_i'$ :

$$A_1'' = A_1''' = A_1'; A_2'' = A_2''' = -A_2'; A_3'' = A_3''' = A_3' \quad (30a)$$

$$A_4'' = -A_4''' = A_4'; A_5'' = -i A_5''' = A_5'; A_6'' = i A_6''' = -A_6' \quad (30b)$$

$$A_7'' = A_7''' = 0; A_7' = A_7''; A_8' = -A_8'' \quad (30c)$$

Finally, we will have:

$$\bar{\varphi}_1 = \left[ \begin{matrix} A_1' C_1 m \pi e^{\lambda_1 X_2} + A_2' C_1 m \pi e^{-\lambda_1 X_2} + A_3' C_2 m \pi e^{\lambda_2 X_2} + A_4' C_2 m \pi e^{-\lambda_2 X_2} \\ + A_5' C_3 m \pi e^{i \lambda_3 X_2} + A_6' C_3 m \pi e^{-i \lambda_3 X_2} + A_7' \lambda_4 e^{\lambda_4 X_2} + A_8' \lambda_4 e^{-\lambda_4 X_2} \end{matrix} \right] \cos(m \pi X_1) \quad (31a)$$

$$\bar{\varphi}_2 = \left[ \begin{matrix} A_1'' C_1 \lambda_4 e^{\lambda_4 X_2} - A_2'' C_1 \lambda_4 e^{-\lambda_4 X_2} + A_3'' C_2 \lambda_2 e^{\lambda_2 X_2} - A_4'' C_2 \lambda_2 e^{-\lambda_2 X_2} \\ + i A_5'' C_3 \lambda_3 e^{i \lambda_3 X_2} - i A_6'' C_3 \lambda_3 e^{-i \lambda_3 X_2} + A_7'' m \pi e^{\lambda_4 X_2} - A_8'' m \pi e^{-\lambda_4 X_2} \end{matrix} \right] \sin(m \pi X_1) \quad (31b)$$

$$\bar{w} = \left[ \begin{matrix} A_1''' e^{\lambda_1 X_2} + A_2''' e^{-\lambda_1 X_2} + A_3''' e^{\lambda_2 X_2} + A_4''' e^{-\lambda_2 X_2} \\ + A_5''' e^{i \lambda_3 X_2} + A_6''' e^{-i \lambda_3 X_2} \end{matrix} \right] \sin(m \pi X_1) \quad (31c)$$

In above equations, sentences with even indexes show a wave that moves in the positive direction of  $X_2$  axis and sentences with odd indexes show a wave that moves in the negative direction of  $X_2$  axis.

According to what was said, we can write:

$$a^+(x) = \left\{ \begin{matrix} A_2' e^{-\lambda_1 X_2} \\ A_4' e^{-\lambda_2 X_2} \\ A_6' e^{-i \lambda_3 X_2} \\ A_8' e^{-\lambda_4 X_2} \end{matrix} \right\}; \quad a^-(x) = \left\{ \begin{matrix} A_1' e^{\lambda_1 X_2} \\ A_3' e^{\lambda_2 X_2} \\ A_5' e^{i \lambda_3 X_2} \\ A_7' e^{\lambda_4 X_2} \end{matrix} \right\} \quad (32)$$

#### 4 Propagation Matrix

Consider two points on the plate a distance  $X^0$  apart in  $X_2$  direction as shown in figure 2. Positive- and negative-going waves propagate from one point to another. Denoting them as Eqs. (32), they are related by:

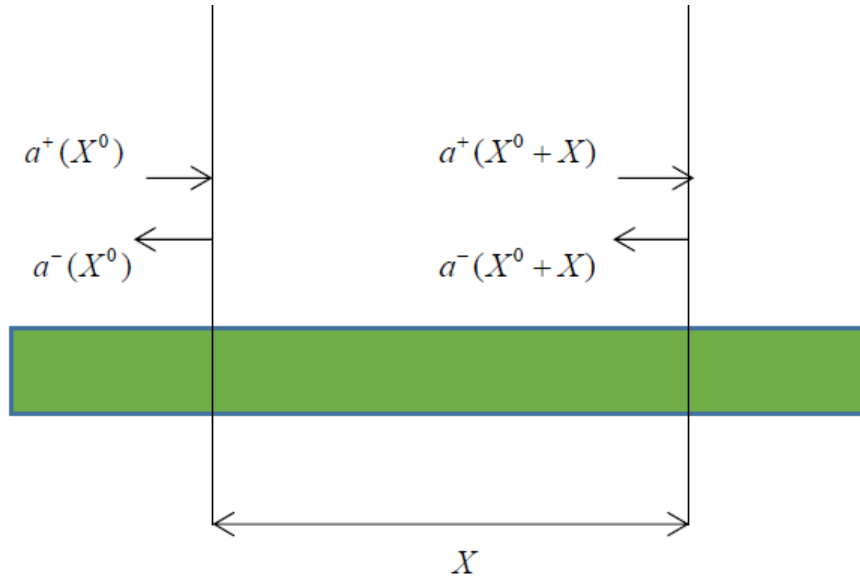


Figure 2 A lateral view of Reddy plate representing positive and negative going propagating waves

$$\begin{aligned} a^+(X + X^0) &= f^+(X) a^+(X^0), \\ a^-(X^0) &= f^-(X) a^-(X + X^0) \end{aligned} \quad (33)$$

In which  $f^+(X)$  is the propagation matrix in the positive direction and  $f^-(X)$  is the propagation matrix in the negative direction. By substituting the wave domain equations in equations above, we will have:

$$f^+(X) = f^-(X) = \begin{bmatrix} e^{-\lambda_1 \delta X_2} & 0 & 0 & 0 \\ 0 & e^{-\lambda_2 \delta X_2} & 0 & 0 \\ 0 & 0 & e^{-i \lambda_3 \delta X_2} & 0 \\ 0 & 0 & 0 & e^{-\lambda_4 \delta X_2} \end{bmatrix} \quad (34)$$

As it is seen, the propagation functions in the positive and negative directions are equal to each other and they are called  $f(X)$ . This is a property which cannot be appeared in non-uniform plates and in them; the propagation matrices are different from each other in the positive and negative directions.

## 5 Reflection Matrix

When the propagated waves in the plate are collided to the boundaries, they are reflected and this action obviously presents that as long as the plate is vibrating, positive and negative waves are propagating in the environment.

Equation between positive and negative travelling waves with the reflection matrix  $r$  will be provided:

$$a^- = r a^+ \quad (35)$$

For obtaining the reflection of waves in the boundaries, the boundary conditions will be used. For two boundary modes of simply supported and clamped, we try to express the reflection of the propagated waves in the plate.

### 5.1 Reflection matrix for the simply support boundary condition

In this case, the boundary conditions, as previously said, are as follows:

$$\overline{M}_2 = \overline{\varphi}_1 = \overline{w} = \overline{P}_2 = 0 \quad (36)$$

The incoming wave to this boundary is called  $a^+$  and the reflected wave from the boundary is called  $a^-$ .

$$\begin{aligned} \overline{M}_2 &= \left[ \frac{1}{60} \pi^4 m^2 \nu - \frac{1}{15} C_1 \pi^2 m^2 \nu - \frac{1}{60} \lambda_1^2 + \frac{1}{15} C_1 \lambda_1^2 \right] a_1^- \\ &+ \left[ \frac{1}{60} \pi^4 m^2 \nu - \frac{1}{15} C_1 \pi^2 m^2 \nu - \frac{1}{60} \lambda_1^2 + \frac{1}{15} C_1 \lambda_1^2 \right] a_1^+ \\ &+ \left[ \frac{1}{60} \pi^4 m^2 \nu - \frac{1}{15} C_2 \pi^2 m^2 \nu - \frac{1}{60} \lambda_2^2 + \frac{1}{15} C_2 \lambda_2^2 \right] a_2^- \\ &+ \left[ \frac{1}{60} \pi^4 m^2 \nu - \frac{1}{15} C_2 \pi^2 m^2 \nu - \frac{1}{60} \lambda_2^2 + \frac{1}{15} C_2 \lambda_2^2 \right] a_2^+ \\ &+ \left[ \frac{1}{60} \pi^4 m^2 \nu - \frac{1}{15} C_3 \pi^2 m^2 \nu - \frac{1}{60} \lambda_3^2 + \frac{1}{15} C_3 \lambda_3^2 \right] a_3^- \\ &+ \left[ \frac{1}{60} \pi^4 m^2 \nu - \frac{1}{15} C_3 \pi^2 m^2 \nu - \frac{1}{60} \lambda_3^2 + \frac{1}{15} C_3 \lambda_3^2 \right] a_3^+ \\ &+ \left[ \frac{1}{60} \pi^4 m^2 \nu - \frac{1}{15} \lambda_4 m \pi \nu + \frac{1}{15} \lambda_4 m \pi \right] a_4^- \\ &+ \left[ \frac{1}{60} \pi^4 m^2 \nu - \frac{1}{15} \lambda_4 m \pi \nu + \frac{1}{15} \lambda_4 m \pi \right] a_4^+ \end{aligned} \quad (37a)$$

$$\bar{\varphi}_1 = \begin{bmatrix} C_1 m \pi a_1^- + C_1 m \pi a_1^+ + C_2 m \pi a_2^- + C_2 m \pi a_2^+ \\ + C_3 m \pi a_3^- + C_3 m \pi a_3^+ + \lambda_4 a_4^- + \lambda_4 a_4^+ \end{bmatrix} = 0 \quad (37b)$$

$$\bar{w} = [a_1^- + a_1^+ + a_2^- + a_2^+ + a_3^- + a_3^+] = 0 \quad (37c)$$

$$\begin{aligned} \bar{P}_2 = & \left[ \frac{1}{336} \pi^2 m^2 \nu - \frac{1}{105} C_1 \pi^2 m^2 \nu + \frac{1}{105} C_1 \lambda_1^2 - \frac{1}{336} \lambda_1^2 \right] a_1^- \\ & + \left[ \frac{1}{336} \pi^2 m^2 \nu - \frac{1}{105} C_1 \pi^2 m^2 \nu + \frac{1}{105} C_1 \lambda_1^2 - \frac{1}{336} \lambda_1^2 \right] a_1^+ \\ & + \left[ \frac{1}{336} \pi^2 m^2 \nu - \frac{1}{105} C_2 \pi^2 m^2 \nu + \frac{1}{105} C_2 \lambda_2^2 - \frac{1}{336} \lambda_2^2 \right] a_2^- \\ & + \left[ \frac{1}{336} \pi^2 m^2 \nu - \frac{1}{105} C_2 \pi^2 m^2 \nu + \frac{1}{105} C_2 \lambda_2^2 - \frac{1}{336} \lambda_2^2 \right] a_2^+ \\ & + \left[ \frac{1}{336} \pi^2 m^2 \nu - \frac{1}{105} C_3 \pi^2 m^2 \nu + \frac{1}{105} C_3 \lambda_3^2 - \frac{1}{336} \lambda_3^2 \right] a_3^- \\ & + \left[ \frac{1}{336} \pi^2 m^2 \nu - \frac{1}{105} C_3 \pi^2 m^2 \nu + \frac{1}{105} C_3 \lambda_3^2 - \frac{1}{336} \lambda_3^2 \right] a_3^+ \\ & + \left[ -\frac{1}{105} \lambda_4 m \pi \nu + \frac{1}{105} \lambda_4 m \pi \right] a_4^- + \left[ -\frac{1}{105} \lambda_4 m \pi \nu + \frac{1}{105} \lambda_4 m \pi \right] a_4^+ \end{aligned} \quad (37d)$$

That by writing it in the form of matrix, the reflection matrix for the simply supported mode is:

$$r_s = A^{-1} B \quad (38)$$

$$r_s = - \begin{bmatrix} A_{11} & A_{12} & A_{13} & A_{14} \\ C_1 m \pi & C_2 m \pi & C_3 m \pi & \lambda_4 \\ 1 & 1 & 1 & 0 \\ A_{41} & A_{42} & A_{43} & A_{44} \end{bmatrix}^{-1} \begin{bmatrix} B_{11} & B_{12} & B_{13} & B_{14} \\ C_1 m \pi & C_2 m \pi & C_3 m \pi & \lambda_4 \\ 1 & 1 & 1 & 0 \\ B_{41} & B_{42} & B_{43} & B_{44} \end{bmatrix} \quad (39)$$

In which:

$$A_{11} = B_{11} = \left[ \frac{1}{60} \pi^4 m^2 \nu - \frac{1}{15} C_1 \pi^2 m^2 \nu - \frac{1}{60} \lambda_1^2 + \frac{1}{15} C_1 \lambda_1^2 \right] \quad (40a)$$

$$A_{12} = B_{12} = \left[ \frac{1}{60} \pi^4 m^2 \nu - \frac{1}{15} C_2 \pi^2 m^2 \nu - \frac{1}{60} \lambda_2^2 + \frac{1}{15} C_2 \lambda_2^2 \right] \quad (40b)$$

$$A_{13} = B_{14} = \left[ \frac{1}{60} \pi^4 m^2 \nu - \frac{1}{15} C_3 \pi^2 m^2 \nu - \frac{1}{60} \lambda_3^2 + \frac{1}{15} C_3 \lambda_3^2 \right] \quad (40c)$$

$$A_{14} = B_{14} = \left[ \frac{1}{60} \pi^4 m^2 \nu - \frac{1}{15} \lambda_4 m \pi \nu + \frac{1}{15} \lambda_4 m \pi \right] \quad (40d)$$

$$A_{41} = B_{41} = \left[ \frac{1}{336} \pi^2 m^2 \nu - \frac{1}{105} C_1 \pi^2 m^2 \nu + \frac{1}{105} C_1 \lambda_1^2 - \frac{1}{336} \lambda_1^2 \right] \quad (40e)$$

$$A_{42} = B_{42} = \left[ \frac{1}{336} \pi^2 m^2 \nu - \frac{1}{105} C_2 \pi^2 m^2 \nu + \frac{1}{105} C_2 \lambda_2^2 - \frac{1}{336} \lambda_2^2 \right] \quad (40f)$$

$$A_{43} = B_{43} = \left[ \frac{1}{336} \pi^2 m^2 \nu - \frac{1}{105} C_3 \pi^2 m^2 \nu + \frac{1}{105} C_3 \lambda_3^2 - \frac{1}{336} \lambda_3^2 \right] \quad (40g)$$

$$A_{44} = B_{44} = \left[ -\frac{1}{105} \lambda_4 m \pi \nu + \frac{1}{105} \lambda_4 m \pi \right] \quad (40h)$$

In this case, this matrix will be a negative identity matrix, that is:

$$r_s = -I \quad (41)$$

### 5.2 Reflection matrix for the Clamped boundary condition

In the clamped mode, the boundary condition is as follows:

$$\bar{\varphi}_1 = \bar{\varphi}_2 = \bar{w} = \bar{w}_{,2} = 0 \quad (42)$$

$$\bar{\varphi}_1 = \begin{bmatrix} C_1 m \pi a_1^- + C_1 m \pi a_1^+ + C_2 m \pi a_2^- + C_2 m \pi a_2^+ \\ + C_3 m \pi a_3^- + C_3 m \pi a_3^+ + \lambda_4 a_4^- + \lambda_4 a_4^+ \end{bmatrix} = 0 \quad (43a)$$

$$\bar{\varphi}_2 = \begin{bmatrix} C_1 \lambda_1 a_1^- - C_1 \lambda_1 a_1^+ + C_2 \lambda_2 a_2^- - C_2 \lambda_2 a_2^+ \\ + i C_3 \lambda_3 a_3^- - i C_3 \lambda_3 a_3^+ + m \pi a_4^- - m \pi a_4^+ \end{bmatrix} = 0 \quad (43b)$$

$$\bar{w} = [a_1^- + a_1^+ + a_2^- + a_2^+ + a_3^- + a_3^+] = 0 \quad (43c)$$

$$\bar{w}_{,2} = [\lambda_1 a_1^- - \lambda_1 a_1^+ + \lambda_2 a_2^- - \lambda_2 a_2^+ + i \lambda_3 a_3^- - i \lambda_3 a_3^+] = 0 \quad (43d)$$

Therefore, the reflection matrix for the clamped mode is as follows:

$$r_C = - \begin{bmatrix} 1 & 1 & 1 & 0 \\ C_1 m \pi & C_2 m \pi & C_3 m \pi & \lambda_4 \\ C_1 \lambda_1 & C_2 \lambda_2 & C_3 i \lambda_3 & m \pi \\ \lambda_1 & \lambda_2 & i \lambda_3 & 0 \end{bmatrix}^{-1} \begin{bmatrix} 1 & 1 & 1 & 0 \\ C_1 m \pi & C_2 m \pi & C_3 m \pi & \lambda_4 \\ -C_1 \lambda_1 & -C_2 \lambda_2 & -C_3 i \lambda_3 & -m \pi \\ -\lambda_1 & -\lambda_2 & -i \lambda_3 & 0 \end{bmatrix} \quad (44)$$

$$\begin{bmatrix} -I & r_A & 0 & 0 \\ f(L) & 0 & -I & 0 \\ 0 & -I & 0 & f(L) \\ 0 & 0 & r_B & -I \end{bmatrix} \begin{bmatrix} a^+ \\ a^- \\ b^+ \\ b^- \end{bmatrix} = 0 \quad (47)$$

And for having determinant answer, this matrix must be zero. By equalizing the determinant of this matrix to zero, the frequency and critical buckling load characteristic equation of the system will be obtained.

### 6 Analyzing the free vibrations of the Reddy plate

Consider the plate shown in Figure 2. For analyzing this plate using our wave method, two wave domains for the positive travelling wave and two wave domains for the negative travelling wave in the direction of  $X_2$  at two beginning and ending points are considered. These waves can be related to each other using the obtained propagation and reflection matrices.

$$b^+ = f(L)a^+; a^- = f(L)b^- \quad (45)$$

In which  $f(L)$  is the propagation matrix of the wave between two points of A and B. Also, using the propagation and reflection equations in the boundaries, we will have:

$$a^+ = r_A a^-; b^- = r_B b^+ \quad (46)$$

In which  $r_A$  and  $r_B$  are the reflection matrices in the boundaries A and B, respectively.

By writing equations in the form of matrix, we have:

### 7. Results and Discussion

For the validation of the results, the values obtained from the wave propagation method and the results obtained from the research literature are compared. Here, the letters S and C representing the simply supported and clamped boundary conditions. For example, in the SCSC boundary condition, the edges along  $x = 0$  and  $x = a$  are simply supported boundary conditions and the edges along  $y = 0$  and  $y = b$  are clamped boundary conditions. The values of  $n$  and  $m$  represented the vibrational modes has  $n$  and  $m$  half-wave in  $x$  and  $y$  directions, respectively. For all modes, the Poisson coefficient  $\nu$  is assumed to be 0.3.

The procedure for obtaining the plate frequencies is specified by the wave propagation method is shown in Figure 3. The plot of the real and imaginary part changes of the determinants of equation (47) in terms of the dimensionless frequency for the SCSC boundary condition and assuming  $m = 1, \delta = 1, \xi = 0$  and  $\tau = 0.1$  is shown in Figure 3. As shown in the figure, the intersection of the real and imaginary curves of the determinant with the zero axis represents the roots of the determinant and hence the frequency of the plate. Furthermore, on the left of the frequency there is another root which is the cut-off frequency in which there is no sign change in the real and imaginary curves.

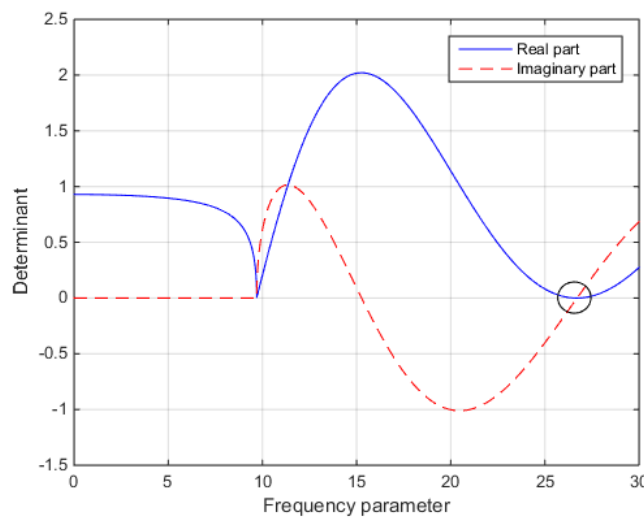


Figure 3 Real and imaginary parts of determinant of Eq. (47) (N=0)

In Table 1, the dimensionless frequencies of the wave method are compared with reference results [21] and [10] for simply supported

boundary condition,  $\mu = 0, 1, 2, 3, 4$ ,  $\delta = 1, 2$  and  $\tau = 0.05, 0.1$  are compared and the obtained values indicate the high accuracy

of the wave propagation method. In Tables 2-4, the dimensionless frequency values for four modes and different boundary conditions of SSSS, SCSS and SCSC are listed for different values of nonlocal parameter, aspect ratio and thickness ratio. The values

$\xi = 0, 0.2, 0.4, 0.6$ ,  $\delta = 0.5, 1, 2$  and assumed.

$\tau = 0.05, 0.1, 0.2$  are

**Table 1.** Dimensionless frequency  $\bar{\omega} = \omega a^2 \sqrt{\rho h / D}$  for SSSS nanoplate

method		Nonlocal parameter				
		$\mu = 0$	$\mu = 1$	$\mu = 2$	$\mu = 3$	$\mu = 4$
	$\tau = 0.1 \quad \delta = 1$					
Present		<b>19.0653</b>	<b>17.4253</b>	<b>16.1467</b>	<b>15.1138</b>	<b>14.2566</b>
[21]		19.0653	17.4231	16.1432	15.1094	14.2518
[10]		19.1678	17.5073	16.2157	15.1907	14.3297
	$\tau = 0.05 \quad \delta = 1$					
Present		<b>19.5625</b>	<b>17.8780</b>	<b>16.5651</b>	<b>15.5046</b>	<b>14.6247</b>
[21]		19.5625	17.8774	16.5642	15.5034	14.6234
[10]		19.6695	17.9412	16.6244	15.5545	14.7315
	$\tau = 0.1 \quad \delta = 2$					
Present		<b>12.0675</b>	<b>11.3862</b>	<b>10.8086</b>	<b>10.3109</b>	<b>9.8761</b>
[21]		12.0675	11.3856	10.8076	10.3095	9.8745
[10]		12.1157	11.4187	10.8447	10.3526	9.9016
	$\tau = 0.05 \quad \delta = 2$					
Present		<b>12.2675</b>	<b>11.5745</b>	<b>10.9870</b>	<b>10.4808</b>	<b>10.0386</b>
[21]		12.2675	11.5743	10.9867	10.4804	10.0382
[10]		12.3445	11.6042	11.0281	10.5343	10.1228

**Table 2.** Dimensionless frequency  $\bar{\omega} = \omega a^2 \sqrt{\rho h / D}$  and frequency ratio for SSSS nanoplates

$\tau = \frac{h}{a}$	$\delta = \frac{b}{a}$	(n, m)	Nonlocal parameter			
			$\xi = 0$	$\xi = 0.2$	$\xi = 0.4$	$\xi = 0.6$
0.05	0.5	(1, 1)	48.2699 (1.0000)	27.9996 (0.5801)	16.1910 (0.3354)	11.1480 (0.2310)
		(1, 2)	156.3907 (1.0000)	56.3974 (0.3606)	29.6834 (0.1898)	19.9900 (0.1278)
		(2, 1)	76.2612 (1.0000)	37.4198 (0.4907)	20.6689 (0.2710)	14.0693 (0.1845)
		(2, 2)	181.9487 (1.0000)	61.1069 (0.3358)	31.9340 (0.1755)	21.4739 (0.1180)
0.1	0.5	(1, 1)	45.4869 (1.0000)	26.4101 (0.5806)	15.2767 (0.3358)	10.5194 (0.2313)
		(1, 2)	133.7198 (1.0000)	48.4172 (0.3621)	25.4944 (0.1907)	17.1705 (0.1284)
		(2, 1)	69.8093 (1.0000)	34.3122 (0.4915)	18.9595 (0.2716)	12.9069 (0.1849)
		(2, 2)	152.7532 (1.0000)	51.5506 (0.3375)	26.9521 (0.1764)	18.1255 (0.1187)
0.2	0.5	(1, 1)	38.1883 (1.0000)	22.2526 (0.5827)	12.8876 (0.3375)	8.8772 (0.2325)
		(1, 2)	95.2602 (1.0000)	35.0582 (0.3680)	18.4935 (0.1941)	12.4601 (0.1308)

*Zargaripoor, Nikkhah Bahrami*

		<b>(2, 1)</b>	55.2543 (1.0000)	27.3374 (0.4948)	15.1277 (0.2738)	10.3019 (0.1864)
		<b>(2, 2)</b>	106.3633 (1.0000)	36.6092 (0.3442)	19.1763 (0.1803)	12.9012 (0.1213)
<hr/>						
		<b>(1, 1)</b>	19.5625 (1.0000)	14.6247 (0.7476)	9.5947 (0.4905)	6.8721 (0.3513)
0.05	1	<b>(1, 2)</b>	48.2699 (1.0000)	27.9996 (0.5801)	16.1910 (0.3354)	11.1480 (0.2310)
		<b>(2, 1)</b>	48.2699 (1.0000)	27.9996 (0.5801)	16.1910 (0.3354)	11.1480(0.2310)
		<b>(2, 2)</b>	76.2612 (1.0000)	37.4198 (0.4907)	20.6689 (0.2710)	14.0693 (0.1845)
<hr/>						
		<b>(1, 1)</b>	19.0653 (1.0000)	14.2566 (0.7478)	9.3550 (0.4907)	6.7009 (0.3515)
0.1	1	<b>(1, 2)</b>	45.4869 (1.0000)	26.4101 (0.5806)	15.2767 (0.3358)	10.5194 (0.2313)
		<b>(2, 1)</b>	45.4869 (1.0000)	26.4101 (0.5806)	15.2767 (0.3358)	10.5194 (0.2313)
		<b>(2, 2)</b>	69.8093 (1.0000)	34.3122 (0.4915)	18.9595 (0.2716)	12.9069 (0.1849)
<hr/>						
		<b>(1, 1)</b>	17.4523 (1.0000)	13.0634 (0.7485)	8.5780 (0.4915)	6.1460 (0.3522)
0.2	1	<b>(1, 2)</b>	38.1883 (1.0000)	22.2526 (0.5827)	12.8876 (0.3375)	8.8772 (0.2325)
		<b>(2, 1)</b>	38.1883 (1.0000)	22.2526 (0.5827)	12.8876 (0.3375)	8.8772 (0.2325)
		<b>(2, 2)</b>	55.2543 (1.0000)	27.3374 (0.4948)	15.1277 (0.2738)	10.3019 (0.1864)
<hr/>						
		<b>(1, 1)</b>	12.2675 (1.0000)	10.0386 (0.8183)	7.1142 (0.5799)	5.2595 (0.4287)
0.05	2	<b>(1, 2)</b>	19.5625 (1.0000)	14.6247 (0.7476)	9.5947 (0.4905)	6.8721 (0.3513)
		<b>(2, 1)</b>	41.1622 (1.0000)	25.1605 (0.6113)	14.8283 (0.3602)	10.2624 (0.2493)
		<b>(2, 2)</b>	48.2699 (1.0000)	27.9996 (0.5801)	16.1910 (0.3354)	11.1480 (0.2310)
<hr/>						
		<b>(1, 1)</b>	12.0675 (1.0000)	9.8761 (0.8184)	6.9999 (0.5801)	5.1753 (0.4289)
0.1	2	<b>(1, 2)</b>	19.0653 (1.0000)	14.2566 (0.7478)	9.3550 (0.4907)	6.7009 (0.3515)
		<b>(2, 1)</b>	39.0977 (1.0000)	23.9166 (0.6117)	14.0994 (0.3606)	9.7578 (0.2496)
		<b>(2, 2)</b>	45.4869 (1.0000)	26.4101 (0.5806)	15.2767 (0.3358)	10.5194 (0.2313)
<hr/>						

0.2	2	(1, 1)	11.3717 (1.0000)	9.3111 (0.8188)	6.6025 (0.5806)	4.8826 (0.4294)
		(1, 2)	17.4523 (1.0000)	13.0634 (0.7485)	8.5780 (0.4915)	6.1460 (0.3522)
		(2, 1)	33.4301 (1.0000)	20.5091 (0.6135)	12.1043 (0.3620)	8.3805 (0.2507)
		(2, 2)	38.1883 (1.0000)	22.2526 (0.5827)	12.8876 (0.3375)	8.8772 (0.2325)

Table 3. Dimensionless frequency  $\bar{\omega} = \omega a^2 \sqrt{\rho h / D}$  and frequency ratio for SCSS nanoplates

$\tau = \frac{h}{a}$	$\delta = \frac{b}{a}$	(n, m)	Nonlocal parameter			
			$\xi = 0$	$\xi = 0.2$	$\xi = 0.4$	$\xi = 0.6$
0.05	0.5	(1, 1)	66.2898 (1.0000)	36.9229 (0.5570)	21.0297 (0.3172)	14.4199 (0.2175)
		(1, 2)	187.2540 (1.0000)	65.8462 (0.3516)	34.6336 (0.1850)	23.3262 (0.1246)
		(2, 1)	89.6072 (1.0000)	42.9016 (0.4788)	23.5496 (0.2628)	16.0059 (0.1786)
		(2, 2)	208.9296 (1.0000)	68.5837 (0.3283)	35.7783 (0.1712)	24.0514 (0.1151)
0.1	0.5	(1, 1)	59.4159 (1.0000)	33.3597 (0.5615)	19.0338 (0.3203)	13.0561 (0.2197)
		(1, 2)	151.2530 (1.0000)	53.9784 (0.3569)	28.4121 (0.1878)	19.1382 (0.1265)
		(2, 1)	79.0782 (1.0000)	38.1544 (0.4825)	20.9720 (0.2652)	14.2581 (0.1803)
		(2, 2)	167.1402 (1.0000)	55.6729 (0.3331)	29.0678 (0.1739)	19.5435 (0.1169)
0.2	0.5	(1, 1)	45.3311 (1.0000)	25.9475 (0.5724)	14.8788 (0.3282)	10.2175 (0.2254)
		(1, 2)	101.3727 (1.0000)	37.3604 (0.3685)	19.7069 (0.1944)	13.2800 (0.1310)
		(2, 1)	59.3203 (1.0000)	29.1202 (0.4909)	16.0567 (0.2707)	10.9239 (0.1842)
		(2, 2)	111.3032 (1.0000)	38.3225 (0.3443)	20.0548 (0.1802)	13.4898 (0.1212)
0.05	1	(1, 1)	23.3076 (1.0000)	17.1646 (0.7336)	11.1288 (0.4756)	7.9345 (0.3391)
		(2, 1)	50.3745 (1.0000)	29.0378 (0.5764)	16.7503 (0.3325)	11.5252 (0.2288)
		(1, 2)	56.7682 (1.0000)	32.2541 (0.5682)	18.5313 (0.3264)	12.7413 (0.2244)
		(2, 2)	82.4728 (1.0000)	39.9430 (0.4843)	21.9915 (0.2667)	14.9581 (0.1814)

*Zargaripoor, Nikkhah Bahrami*

---

0.1	1					
		(1, 1)	22.4018 (1.0000)	16.5256 (0.7377)	10.7254 (0.4788)	7.6493 (0.3415)
		(2, 1)	47.1306 (1.0000)	27.2247 (0.5776)	15.7146 (0.3334)	10.8144 (0.2295)
		(1, 2)	52.2324 (1.0000)	29.8128 (0.5708)	17.1459 (0.3283)	11.7911 (0.2257)
		(2, 2)	74.2252 (1.0000)	36.1208 (0.4866)	19.9045 (0.2682)	13.5411 (0.1824)
0.2	1					
		(1, 1)	19.7695 (1.0000)	14.6531 (0.7412)	9.5386 (0.4825)	6.8095 (0.3444)
		(2, 1)	39.0576 (1.0000)	22.6936 (0.5810)	13.1236 (0.3360)	9.0356 (0.2313)
		(1, 2)	41.7851 (1.0000)	24.1293 (0.5775)	13.9182 (0.3331)	9.5775 (0.2292)
		(2, 2)	57.2458 (1.0000)	28.1960 (0.4925)	15.5737 (0.2720)	10.6003 (0.1852)
0.05	2					
		(1, 1)	12.8339 (1.0000)	10.4688 (0.8157)	7.3931 (0.5761)	5.4563 (0.4251)
		(1, 2)	21.2891 (1.0000)	15.7891 (0.7417)	10.2944 (0.4836)	7.3557 (0.3455)
		(2, 1)	41.4323 (1.0000)	25.3002 (0.6106)	14.9038 (0.3597)	10.3132 (0.2489)
		(2, 2)	49.2546 (1.0000)	28.4781 (0.5782)	16.4467 (0.3339)	11.3200 (0.2298)
0.1	2					
		(1, 1)	12.5937 (1.0000)	10.2762 (0.8160)	7.2594 (0.5764)	5.3584 (0.4255)
		(1, 2)	20.6182 (1.0000)	15.3064 (0.7424)	9.9858 (0.4843)	7.1366 (0.3461)
		(2, 1)	39.3163 (1.0000)	24.0301 (0.6112)	14.1606 (0.3602)	9.7999 (0.2493)
		(2, 2)	46.2637 (1.0000)	26.7892 (0.5791)	15.4788 (0.3346)	10.6552 (0.2303)
0.2	2					
		(1, 1)	11.7827 (1.0000)	9.6247 (0.8169)	6.8062 (0.5776)	5.0261 (0.4266)
		(1, 2)	18.5563 (1.0000)	13.8157 (0.7445)	9.0302 (0.4866)	6.4577 (0.3480)
		(2, 1)	33.5542 (1.0000)	20.5746 (0.6132)	12.1395 (0.3617)	8.4041 (0.2504)
		(2, 2)	38.6067 (1.0000)	22.4614 (0.5818)	12.9983 (0.3367)	8.9513 (0.2319)

---

**Table 4.** Dimensionless frequency  $\bar{\omega} = \omega a^2 \sqrt{\rho h / D}$  and frequency ratio for SCSC nanoplates

$\tau = \frac{h}{a}$	$\delta = \frac{b}{a}$	$(n, m)$	Nonlocal parameter			
			$\xi = 0$	$\xi = 0.2$	$\xi = 0.4$	$\xi = 0.6$
0.05	0.5	(1, 1)	88.5692 (1.0000)	48.3921 (0.5464)	27.3718 (0.3090)	18.7341 (0.2115)
		(1, 2)	219.3453 (1.0000)	74.5856 (0.3400)	38.9573 (0.1776)	26.1925 (0.1194)
		(2, 1)	106.8335 (1.0000)	50.4645 (0.4724)	27.6125 (0.2585)	18.7531 (0.1755)
		(2, 2)	237.6635 (1.0000)	76.1353 (0.3203)	38.5753 (0.1665)	26.5823 (0.1118)
0.1	0.5	(1, 1)	75.2832 (1.0000)	41.6212 (0.5529)	23.5827 (0.3133)	16.1444 (0.2144)
		(1, 2)	167.8807 (1.0000)	58.5725 (0.3489)	30.6465 (0.1825)	20.6115 (0.1228)
		(2, 1)	90.1355 (1.0000)	43.0810 (0.4780)	23.6146 (0.2620)	16.0436 (0.1780)
		(2, 2)	181.3243 (1.0000)	59.5150 (0.3282)	30.9836 (0.1709)	20.8174 (0.1148)
0.2	0.5	(1, 1)	53.1087 (1.0000)	30.1629 (0.5679)	17.1903 (0.3237)	11.7824 (0.2219)
		(1, 2)	106.7070 (1.0000)	39.3108 (0.3684)	20.6535 (0.1936)	13.9020 (0.1303)
		(2, 1)	63.8945 (1.0000)	31.3079 (0.4900)	17.2314 (0.2697)	11.7171 (0.1834)
		(2, 2)	115.9685 (1.0000)	40.0078 (0.3450)	20.8984 (0.1802)	14.0507 (0.1212)
0.05	1	(1, 1)	28.3174 (1.0000)	20.6724 (0.7300)	13.3181 (0.4703)	9.4734 (0.3345)
		(2, 1)	53.0989 (1.0000)	30.4637 (0.5737)	17.5426 (0.3304)	12.0648 (0.2272)
		(1, 2)	66.2898 (1.0000)	36.9229 (0.5570)	21.0297 (0.3172)	14.4199 (0.2175)
		(2, 2)	89.6072 (1.0000)	42.9016 (0.4788)	23.5496 (0.2628)	16.0059 (0.1786)
0.1	1	(1, 1)	26.7084 (1.0000)	19.5537 (0.7321)	12.6161 (0.4724)	8.9777 (0.3361)
		(2, 1)	49.1756 (1.0000)	28.3017 (0.5755)	16.3127 (0.3317)	11.2215 (0.2282)
		(1, 2)	59.4159 (1.0000)	33.3597 (0.5615)	19.0338 (0.3203)	13.0561 (0.2197)
		(2, 2)	79.0783 (1.0000)	38.1544 (0.4825)	20.9720 (0.2652)	14.2581 (0.1803)

0.2	1					
		(1, 1)	22.5355 (1.0000)	16.6210 (0.7375)	10.7703 (0.4779)	7.6740 (0.3405)
		(2, 1)	40.0654 (1.0000)	23.2394 (0.5800)	13.4266 (0.3351)	9.2416 (0.2307)
		(1, 2)	45.3350 (1.0000)	25.9475 (0.5724)	14.8788 (0.3282)	10.2175 (0.2254)
		(2, 2)	59.3313 (1.0000)	29.1202 (0.4908)	16.0567 (0.2706)	10.9239 (0.1841)
0.05	2					
		(1, 1)	13.5772 (1.0000)	11.0475 (0.8137)	7.7813 (0.5731)	5.7357 (0.4224)
		(1, 2)	23.3076 (1.0000)	17.1646 (0.7364)	11.1288 (0.4775)	7.9345 (0.3404)
		(2, 1)	41.7487 (1.0000)	25.4698 (0.6101)	14.9975 (0.3592)	10.3768 (0.2486)
		(2, 2)	50.3746 (1.0000)	29.0378 (0.5764)	16.7503 (0.3325)	11.5252 (0.2288)
0.1	2					
		(1, 1)	13.2747 (1.0000)	10.8073 (0.8141)	7.6159 (0.5737)	5.6149 (0.4230)
		(1, 2)	22.4018 (1.0000)	16.5256 (0.7377)	10.7254 (0.4788)	7.6493 (0.3415)
		(2, 1)	39.5680 (1.0000)	24.1656 (0.6107)	14.2354 (0.3598)	9.8506 (0.2490)
		(2, 2)	47.1306 (1.0000)	27.2247 (0.5776)	15.7146 (0.3334)	10.8144 (0.2295)
0.2	2					
		(1, 1)	12.2939 (1.0000)	10.0250 (0.8154)	7.0754 (0.5755)	5.2198 (0.4246)
		(1, 2)	19.7696 (1.0000)	14.6531 (0.7412)	9.5386 (0.4825)	6.8095 (0.3444)
		(2, 1)	33.6918 (1.0000)	20.6502 (0.6129)	12.1811 (0.3615)	8.4322 (0.2503)
		(2, 2)	39.0576 (1.0000)	22.6936 (0.5810)	13.1236 (0.3360)	9.0356 (0.2313)

Figure 4 illustrates the plot of frequency ratio changes based on thickness to length ratio for different values of the aspect ratio  $\delta$  for three boundary conditions of SSSS, SCSS and SCSC and for  $\xi = 0.6$ . Regarding the figures, by increasing the thickness to length ratio, the frequency ratio for different values of  $\delta$  increases, Also, the increase rate of frequency ratio is low for larger values of  $\delta$ . As it can be observed, the SCSC boundary condition has the highest and SSSS has the lowest increase rate of frequency ratio. Figure 5 shows the plot of frequency ratio changes based on the nonlocal parameter for different values of aspect ratio and for SCSC boundary condition and  $\tau = 0.1$ . As it can be observed, by increasing the nonlocal parameter the values of frequency ratio decrease. Also, the influence of nonlocal parameter is more considerable for lower values of aspect ratio. The plot of frequency ratio changes based on nonlocal parameter for different modes number of the above boundary conditions and for  $\delta = 1$  and  $\tau = 0.1$  is drawn in Figure 6. It is observed that for higher modes, the frequency reduction rate is higher. Variations of frequency ratio with nonlocal parameter for different boundary

conditions and for  $\tau = 0.2$  and  $\delta = 0.5$  is shown in figure 7. As it can be seen, the values of frequency ratio decrease by increasing the values of nonlocal parameter. In addition, the influence of nonlocal parameter is more remarkable for SCSC boundary condition. The method for obtaining the critical buckling load is the same as the method of obtaining a non-dimensional frequency, with the difference that the real and imaginary part of the determinant are plotted in terms of different values of dimensionless critical buckling load  $N$  and for  $\beta = 0$  (As shown in Figure 8). In order to verify the critical buckling load obtained from the wave propagation method, in Table 5, the critical load values of the boundary conditions for simply supported boundary condition and different values of nonlocal parameter and for  $\xi = 0, 0.1, 0.2, 0.3, \delta = 1, 2$  and  $\tau = 0.1$  are compared with the results obtained from [21]. It can be observed that the values obtained by the present method are very close to [21]. In Table 6, the critical loads of the first mode for the three boundary conditions of SSSS, SCSS and SCSC are listed for different values of nonlocal parameter, aspect ratio and thickness to length ratio.

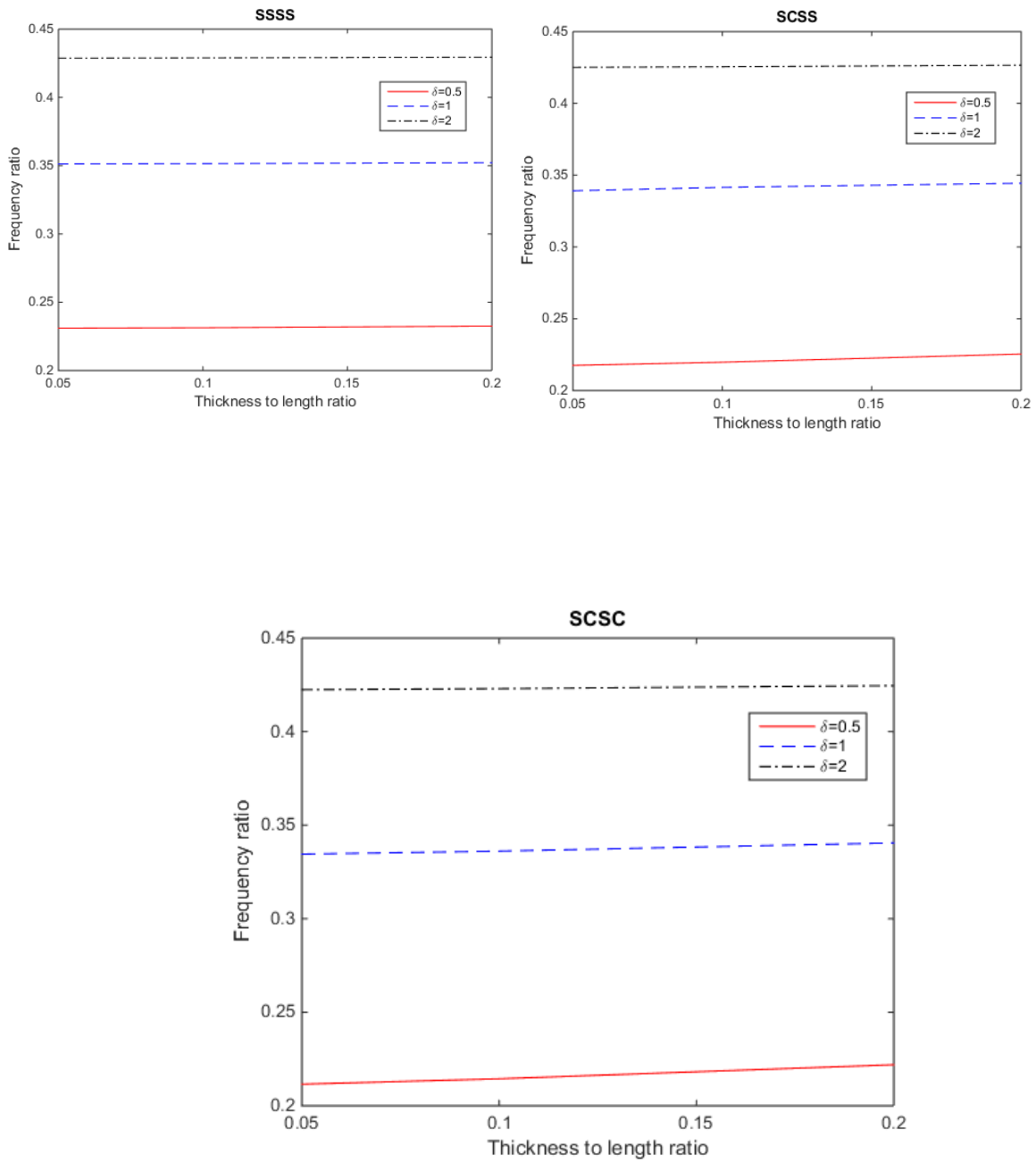


**Figure 4** Variations of frequency ratio with thickness to length ratio for different boundary conditions and values of aspect ratio ( $\xi = 0.6$ )

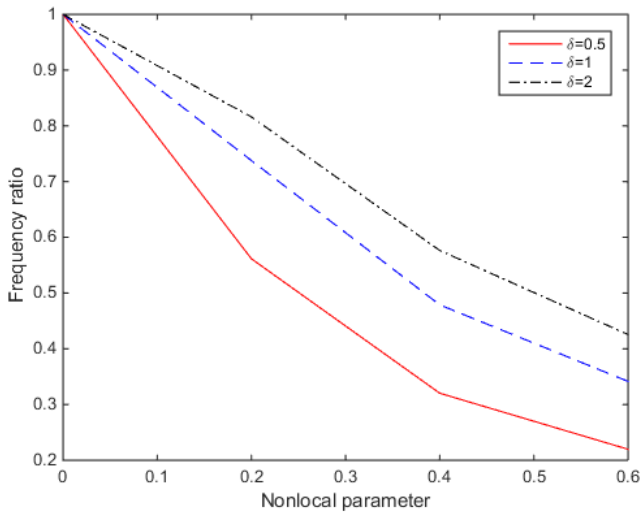


Figure 5 Variations of frequency ratio with nonlocal parameter for different values of aspect ratio (SCSC,  $\tau = 0.1$ )

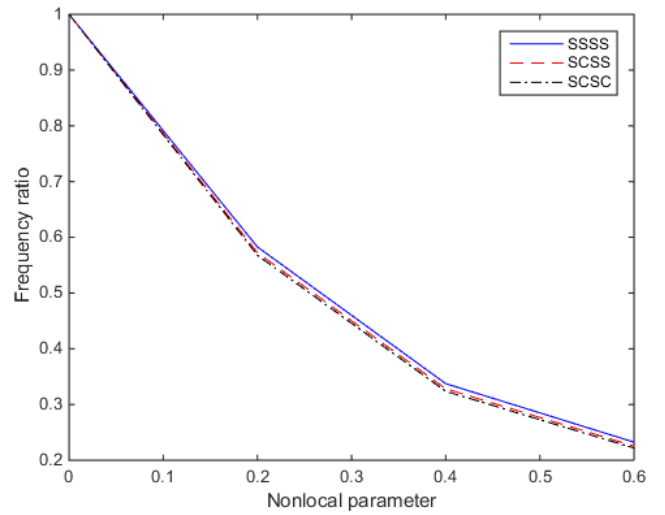


Figure 7 Variations of frequency ratio with nonlocal parameter for different boundary conditions ( $\tau = 0.2$ ,  $\delta=0.5$ )

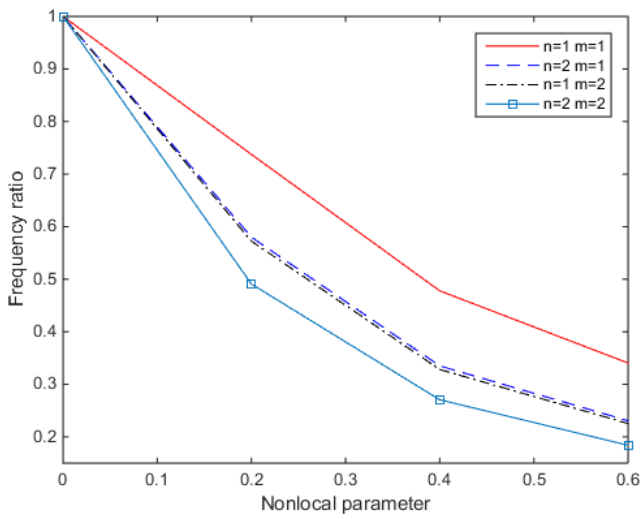


Figure 6 Variations of frequency ratio with nonlocal parameter for different mode numbers (SCSC,  $\tau = 0.2$ ,  $\delta=1$ )

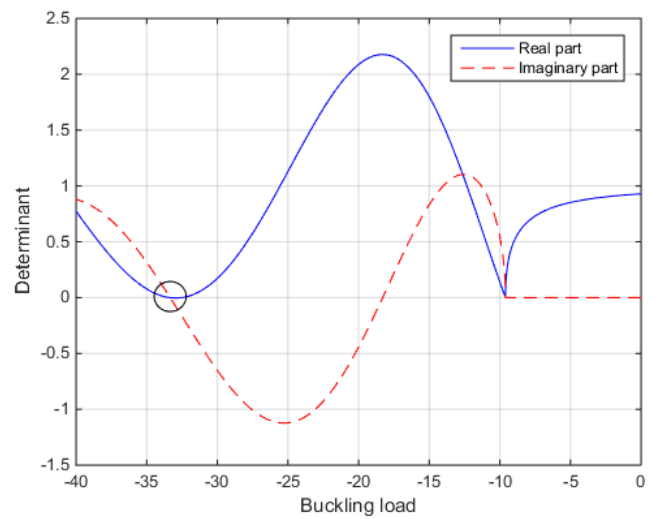


Figure 8 Real and imaginary parts of determinant of Eq. (47) ( $\beta = 0$ )

**Table 5.** Dimensionless buckling load  $N = \frac{a^2}{D} N_{xx}$  ratio for SSSS nanoplate and different nonlocal parameters

$\tau = \frac{h}{a}$	$\delta = \frac{b}{a}$	Method	Nonlocal parameter			
			$\xi = 0$	$\xi = 0.1$	$\xi = 0.2$	$\xi = 0.3$
0.1	1	Present	<b>-18.6861</b>	<b>-15.6057</b>	<b>-10.4417</b>	<b>-6.7300</b>
		[21]	-18.6861	-15.6057	-10.4408	-6.7200
0.1	2	Present	<b>-11.9171</b>	<b>-10.6084</b>	<b>-7.9795</b>	<b>-5.6470</b>
		[21]	-11.9171	-10.6084	-7.9794	-6.7289

**Table 6.** Dimensionless buckling load  $N = \frac{a^2}{D} N_{xx}$  and buckling load ratio for different nonlocal parameters and boundary conditions

$\tau = \frac{h}{a}$	$\delta = \frac{b}{a}$		Nonlocal parameter			
			$\xi = 0$	$\xi = 0.1$	$\xi = 0.2$	$\xi = 0.3$
0.05	0.5	SSSS	-47.6685 (1.0000)	-31.9178 (0.6695)	-16.0288 (0.3362)	-8.7605 (0.1837)
		SCSS	-79.5633 (1.0000)	-42.8457 (0.5385)	-17.5740 (0.2208)	-9.2180 (0.1158)
		SCSC	-134.9581 (1.0000)	-53.1381 (0.3937)	-19.1887 (0.1421)	-9.2576 (0.0685)
0.1	0.5	SSSS	-43.2593 (1.0000)	-28.9651 (0.6695)	-14.5461 (0.3362)	-7.9501 (0.1837)
		SCSS	-66.7824 (1.0000)	-36.3659 (0.5445)	-15.2557 (0.2284)	-7.7511 (0.1160)
		SCSC	-102.7726 (1.0000)	-41.0587 (0.3995)	-14.6297 (0.1423)	-7.0586 (0.0686)
0.2	0.5	SSSS	-31.6290 (1.0000)	-21.1779 (0.6695)	-10.6354 (0.3362)	-5.8127(0.1837)
		SCSS	-41.2908 (1.0000)	-22.5930 (0.5471)	-9.4627 (0.2291)	-4.8110 (0.1165)
		SCSC	-53.6786 (1.0000)	-21.4606 (0.3997)	-7.6495 (0.1425)	-3.6909 (0.0687)
0.05	1					

0.1	1	SSSS	-19.4649 (1.0000)	-16.2560 (0.8351)	-10.8768 (0.5588)	-7.0105 (0.3601)
		SCSS	-25.7204 (1.0000)	-20.3659 (0.7917)	-12.5347 (0.4872)	-7.6406 (0.2970)
		SCSC	-36.5557 (1.0000)	-26.0954 (0.7138)	-14.2750 (0.3905)	-8.2991 (0.2270)
0.2	1	SSSS	-18.6861 (1.0000)	-15.6057 (0.8351)	-10.4417 (0.5588)	-6.7300 (0.3601)
		SCSS	-24.1988 (1.0000)	-19.1600 (0.7917)	-11.7901 (0.4872)	-7.1885 (0.2970)
		SCSC	-33.3404 (1.0000)	-23.9021 (0.7170)	-13.2886 (0.3985)	-7.6286 (0.2288)
0.2	1	SSSS	-16.1139 (1.0000)	-13.4575 (0.8351)	-9.0043 (0.5588)	-5.8035 (0.3601)
		SCSS	-19.6873 (1.0000)	-15.6056 (0.7926)	-9.6167 (0.4884)	-5.9067 (0.3000)
		SCSC	-24.9667 (1.0000)	-18.2174 (0.7296)	-10.0571 (0.4028)	-5.7268 (0.2293)

Regarding the table 6, by increasing the thickness to length ratio, the buckling load ratio for different values of  $\delta$  increases. Also, by increasing the nonlocal parameter the values of buckling load ratio decrease. In addition, the influence of nonlocal parameter is more remarkable for SCSC boundary condition.

### 8. Conclusion

This paper presents the free vibration and buckling analysis of the rectangular Reddy nanoplates based on nonlocal elasticity theory using wave propagation method. Dimensionless natural frequencies and dimensionless buckling load of the nanoplate are compared with available literature and excellent agreement is observed. In future works, these results can be an excellent database to verify approximate or other analytical solutions as they are regarded as exact solutions. Also, it is seen that the computer coding of the proposed method is much easier than the classical methods which makes it more appropriate in implementation. Moreover, the influence of different parameters, such as nonlocal parameter, aspect ratio, aspect of length to thickness of nanoplate and boundary conditions are discussed. It was observed that:

- By increasing the thickness to length ratio, the frequency ratio and buckling load ratio for different values of  $\delta$  increase.
- By increasing the nonlocal parameter the values of frequency ratio and buckling load ratio decrease.
- By increasing the nonlocal parameter, the frequency reduction rate is higher for higher modes.
- The influence of nonlocal parameter is more remarkable for SCSC boundary condition.

### References

1. Mindlin, R. and H. Tiersten, *Effects of couple-stresses in linear elasticity*. Archive for Rational Mechanics and analysis, 1962. **11**(1): p. 415-448.
2. Mindlin, R.D., *Micro-structure in linear elasticity*. Archive for Rational Mechanics and Analysis, 1964. **16**(1): p. 51-78.
3. Eringen, A.C., *Theory of micromorphic materials with memory*. International Journal of Engineering Science, 1972. **10**(7): p. 623-641.
4. Eringen, A.C., *Nonlocal continuum field theories*. 2002: Springer Science & Business Media.
5. Makvandi, H., et al., *A new approach for nonlinear vibration analysis of thin and moderately thick rectangular plates under inplane compressive load*. Journal of Computational Applied Mechanics.
6. Zargaripoor, A., Bahrami, Arian, Nikkhah Bahrami, Mansour, *Free vibration and buckling analysis of third-order shear deformation plate theory using exact wave propagation approach*. Journal of Computational Applied Mechanics, 2018.
7. Javidi, R., M. Moghimi Zand, and K. Dastani, *Dynamics of Nonlinear rectangular plates subjected to an orbiting mass based on shear deformation plate theory*. Journal of Computational Applied Mechanics, 2017.
8. Pradhan, S. and J. Phadikar, *Nonlocal elasticity theory for vibration of nanoplates*. Journal of Sound and Vibration, 2009. **325**(1-2): p. 206-223.

9. Murmu, T. and S. Pradhan, *Small-scale effect on the free in-plane vibration of nanoplates by nonlocal continuum model*. Physica E: Low-dimensional Systems and Nanostructures, 2009. **41**(8): p. 1628-1633.
10. Aghababaei, R. and J. Reddy, *Nonlocal third-order shear deformation plate theory with application to bending and vibration of plates*. Journal of Sound and Vibration, 2009. **326**(1-2): p. 277-289.
11. Aksencer, T. and M. Aydogdu, *Levy type solution method for vibration and buckling of nanoplates using nonlocal elasticity theory*. Physica E: Low-dimensional Systems and Nanostructures, 2011. **43**(4): p. 954-959.
12. Malekzadeh, P. and M. Shojaee, *Free vibration of nanoplates based on a nonlocal two-variable refined plate theory*. Composite Structures, 2013. **95**: p. 443-452.
13. Chakraverty, S. and L. Behera, *Free vibration of rectangular nanoplates using Rayleigh–Ritz method*. Physica E: Low-dimensional Systems and Nanostructures, 2014. **56**: p. 357-363.
14. Malekzadeh, P. and M. Shojaee, *A two-variable first-order shear deformation theory coupled with surface and nonlocal effects for free vibration of nanoplates*. Journal of Vibration and Control, 2015. **21**(14): p. 2755-2772.
15. Chakraverty, S. and L. Behera, *Small scale effect on the vibration of non-uniform nanoplates*. Structural Engineering and Mechanics, 2015. **55**(3): p. 495-510.
16. Panyatong, M., B. Chinnaboon, and S. Chucheepeksakul, *Nonlocal second-order shear deformation plate theory for free vibration of nanoplates*. Suranaree Journal of Science & Technology, 2015. **22**(4).
17. Behera, L. and S. Chakraverty, *Effect of scaling effect parameters on the vibration characteristics of nanoplates*. Journal of Vibration and Control, 2016. **22**(10): p. 2389-2399.
18. Faroughi, S. and S.M.H. Goushegir, *Free in-plane vibration of heterogeneous nanoplates using Ritz method*. Journal of Theoretical and Applied Vibration and Acoustics, 2016. **2**(1): p. 1-20.
19. Shokrani, M.H. and A.R. Shahidi, *Size-dependent free vibration analysis of rectangular nanoplates with the consideration of surface effects using finite difference method*. Journal of applied and computational mechanics, 2015. **1**(3): p. 122-133.
20. Sarrami-Foroushani, S. and M. Azhari, *Nonlocal buckling and vibration analysis of thick rectangular nanoplates using finite strip method based on refined plate theory*. Acta Mechanica, 2016. **227**(3): p. 721-742.
21. Hosseini-Hashemi, S., M. Kermajani, and R. Nazemnezhad, *An analytical study on the buckling and free vibration of rectangular nanoplates using nonlocal third-order shear deformation plate theory*. European Journal of Mechanics-A/Solids, 2015. **51**: p. 29-43.
22. Rong, D., et al., *A New Analytical Approach for Free Vibration, Buckling and Forced Vibration of Rectangular Nanoplates Based on Nonlocal Elasticity Theory*. International Journal of Structural Stability and Dynamics, 2017: p. 1850055.
23. Daneshmehr, A., A. Rajabpoor, and A. Hadi, *Size dependent free vibration analysis of nanoplates made of functionally graded materials based on nonlocal elasticity theory with high order theories*. International Journal of Engineering Science, 2015. **95**: p. 23-35.
24. Hosseini, M., et al., *Size-Dependent Stress Analysis of Single-Wall Carbon Nanotube Based on Strain Gradient Theory*. International Journal of Applied Mechanics, 2017. **9**(06): p. 1750087.
25. Hosseini, M., et al., *Stress analysis of rotating nanodisks of variable thickness made of functionally graded materials*. International Journal of Engineering Science, 2016. **109**: p. 29-53.
26. Nejad, M.Z., A. Rastgoo, and A. Hadi, *Effect of exponentially-varying properties on displacements and stresses in pressurized functionally graded thick spherical shells with using iterative technique*. Journal of Solid Mechanics, 2014. **6**(4): p. 366-377.
27. Nejad, M.Z. and A. Hadi, *Eringen's non-local elasticity theory for bending analysis of bi-directional functionally graded Euler–Bernoulli nano-beams*. International Journal of Engineering Science, 2016. **106**: p. 1-9.
28. Nejad, M.Z. and A. Hadi, *Non-local analysis of free vibration of bi-directional functionally graded Euler–Bernoulli nano-beams*. International Journal of Engineering Science, 2016. **105**: p. 1-11.
29. Nejad, M.Z., A. Hadi, and A. Farajpour, *Consistent couple-stress theory for free vibration analysis of Euler–Bernoulli nano-beams made of arbitrary bi-directional functionally graded materials*. Structural Engineering and Mechanics, 2017. **63**(2): p. 161-169.
30. Nejad, M.Z., A. Hadi, and A. Rastgoo, *Buckling analysis of arbitrary two-directional functionally graded Euler–Bernoulli nano-beams based on nonlocal elasticity theory*. International Journal of Engineering Science, 2016. **103**: p. 1-10.
31. Nejad, M.Z., A. Rastgoo, and A. Hadi, *Exact elastoplastic analysis of rotating disks made of functionally graded materials*. International Journal of Engineering Science, 2014. **85**: p. 47-57.
32. Shishesaz, M., et al., *Analysis of functionally graded nanodisks under thermoelastic loading based on the*

- strain gradient theory. *Acta Mechanica*, 2017. **228**(12): p. 4141-4168.
33. Hadi, A., et al., *Buckling analysis of FGM Euler-Bernoulli nano-beams with 3D-varying properties based on consistent couple-stress theory*. *Steel and Composite Structures*, 2018. **26**(6): p. 663-672.
34. Zamani Nejad, M., M. Jabbari, and A. Hadi, *A review of functionally graded thick cylindrical and conical shells*. *Journal of Computational Applied Mechanics*, 2017. **48**(2): p. 357-370.
35. Hadi, A., M.Z. Nejad, and M. Hosseini, *Vibrations of three-dimensionally graded nanobeams*. *International Journal of Engineering Science*, 2018. **128**: p. 12-23.
36. Zhang, X., G. Liu, and K. Lam, *Vibration analysis of thin cylindrical shells using wave propagation approach*. *Journal of sound and vibration*, 2001. **239**(3): p. 397-403.
37. Mei, C. and B. Mace, *Wave reflection and transmission in Timoshenko beams and wave analysis of Timoshenko beam structures*. *Journal of vibration and acoustics*, 2005. **127**(4): p. 382-394.
38. Natsuki, T., M. Endo, and H. Tsuda, *Vibration analysis of embedded carbon nanotubes using wave propagation approach*. *Journal of Applied Physics*, 2006. **99**(3): p. 034311.
39. Xuebin, L., *Study on free vibration analysis of circular cylindrical shells using wave propagation*. *Journal of sound and vibration*, 2008. **311**(3-5): p. 667-682.
40. Bahrami, A., M.R. Ilkhani, and M.N. Bahrami, *Wave propagation technique for free vibration analysis of annular circular and sectorial membranes*. *Journal of Vibration and Control*, 2015. **21**(9): p. 1866-1872.
41. Bahrami, A. and A. Teimourian, *Nonlocal scale effects on buckling, vibration and wave reflection in nanobeams via wave propagation approach*. *Composite Structures*, 2015. **134**: p. 1061-1075.
42. Ilkhani, M., A. Bahrami, and S. Hosseini-Hashemi, *Free vibrations of thin rectangular nano-plates using wave propagation approach*. *Applied Mathematical Modelling*, 2016. **40**(2): p. 1287-1299.
43. Bahrami, A. and A. Teimourian, *Study on the effect of small scale on the wave reflection in carbon nanotubes using nonlocal Timoshenko beam theory and wave propagation approach*. *Composites Part B: Engineering*, 2016. **91**: p. 492-504.
44. Bahrami, A. and A. Teimourian, *Study on vibration, wave reflection and transmission in composite rectangular membranes using wave propagation approach*. *Meccanica*, 2017. **52**(1-2): p. 231-249.
45. Bahrami, A. and A. Teimourian, *Small scale effect on vibration and wave power reflection in circular annular nanoplates*. *Composites Part B: Engineering*, 2017. **109**: p. 214-226.
46. Bahrami, A., *Free vibration, wave power transmission and reflection in multi-cracked nanorods*. *Composites Part B: Engineering*, 2017. **127**: p. 53-62.
47. Reddy, J.N., *A simple higher-order theory for laminated composite plates*. *Journal of applied mechanics*, 1984. **51**(4): p. 745-752.